Initiation of vacuum insulator surface high-voltage flashover with electrons produced by laser illumination

Ya. E. Krasik and J. G. Leopold
Physics Department, Technion, Haifa 32000, Israel

(Received 20 July 2015; accepted 29 July 2015; published online 14 August 2015)

In this paper, experiments are described in which cylindrical vacuum insulator samples and samples inclined at 45° relative to the cathode were stressed by microsecond timescale high-voltage pulses and illuminated by focused UV laser beam pulses. In these experiments, we were able to distinguish between flashover initiated by the laser producing only photo-electrons and when plasma is formed. It was shown that flashover is predominantly initiated near the cathode triple junction. Even dense plasma formed near the anode triple junction does not necessarily lead to vacuum surface flashover. The experimental results directly confirm our conjecture that insulator surface breakdown can be avoided by preventing its initiation [J. G. Leopold *et al.*, Phys. Rev. ST Accel. Beams **10**, 060401 (2007)] and complement our previous experimental results [J. Z. Gleizer *et al.*, IEEE Trans. Dielectr. Electr. Insul. **21**, 2394 (2014) and J. Z. Gleizer *et al.*, J. Appl. Phys. **117**, 073301 (2015)]. © *2015 AIP Publishing LLC*. [http://dx.doi.org/10.1063/1.4928580]

I. INTRODUCTION

Vacuum surface flashover leading to insulator breakdown is known to be a serious limiting factor in the design of high-voltage pulsed-power systems. This very old and complex problem has been studied for many years, and yet the same serious vacuum insulation problems seem to remain.[4–7]

It is commonly accepted that surface flashover is initiated by charged particles produced by processes occurring on the conducting surfaces of the electrodes as a result of the application of a high electric field. This high electric field, in particular, in the vicinity of triple points (the metal-vacuum-insulator junction), causes electrode micro-protrusions explosion accompanied by the formation of dense plasma. The latter serves as a source of electrons, which accelerate along the component of the applied electric field tangential to the surface of the insulator, causing in turn an avalanche induced by secondary electron emission processes. In addition, this plasma serves also as a source of UV radiation, which could on its own promote surface flashover. All these phenomena result from the experimental limitations related to the smoothness of the electrode surfaces and imperfect vacuum. The dynamics of the electrons emitted from the plasma depends on the magnitude and the orientation of the electric field. We conjectured that by deflecting these primary electrons away from the insulator surface the breakdown properties of the vacuum insulator could be improved.[1] Since we assume that electrons are the most common breakdown initiators, our conjecture excluded anode triple junction (ATJ) initiation. Recently,[2] by measuring the flashover breakdown electric fields over various insulator arrangements using a conditioning method, we experimentally demonstrated that for high voltage pulses of a microsecond time scale duration, initiation is indeed predominantly at the cathode triple junction (CTJ). It was shown that the flashover field increases significantly as the orientation of the electric field is designed such that electrons are accelerated away from the insulator surface. Moreover, we have shown that breakdown initiation does not occur at the ATJ even when the electric fields in that location are very high. These results were further supported by experiments[3] in which we studied the light emitted by the flashover plasma in time and space and we determined the plasma density and temperature by spectroscopic methods.

When the insulator is inclined to 45° at the CTJ and at the same time to 135° at the ATJ, the electric field at the ATJ becomes infinite. Because of this, one of the main conclusions of the experiments by Stygar *et al.*[8] was that the Anderson model[9] for anode-initiated flashover is relevant. This model suggests that the extreme anode electric fields cause the emission of dielectric surface electrons, which in turn cause the development of a sub-surface dielectric breakdown branching toward the cathode, causing catastrophic bulk burnout of the insulator. Also, a recent patent[10] by Lauer and Lauer is devoted to the subject of increased electric field flashover with improved design of the ATJ which is believed to play a crucial role in surface flashover formation.

In addition to the electric field stress and mechanical and vacuum imperfections, the presence of UV light is known to initiate insulator flashover. The influence of UV irradiation on surface flashover at atmospheric pressure[11–15] was studied at Texas Tech University. In the case of vacuum conditions, Enloe and Gilgenbach[16–18] showed that the irradiation of insulators made of different materials with a pulsed excimer laser (249 nm) and power densities in the range (0.4–6) MW/cm^2 leads to induced flashover at electric fields lower than the static breakdown fields and with drastically decreasing time delays of the flashover initiation relative to the application of the high-voltage pulse with increasing radiation power density. The results of these experiments also showed that for a 45° insulator inclination angle relative to the cathode, the breakdown electric field was almost twice that required for the breakdown of insulators inclined at 135° and for the same UV power density.

Vacuum insulator flashover initiated by laser illumination has recently been reexamined.[19–23] In these experiments, UV irradiation of vacuum insulator surfaces with a pulsed laser beam (266 nm) focused to a diameter of 1 mm and having a power density in the range 10^6–10^8 W/cm^2 was used. It was shown that UV radiation affected the flashover processes by decreasing the amplitude of the breakdown voltage from tens of kV to several kV when the laser beam was focused near the CTJ. It was also shown that the irradiation of the insulator by a 532 nm laser beam does not change the amplitude of the breakdown electric field when the insulator is inclined to 45°.

The main purpose of the present research was to experimentally study the influences of primary charged particles generated at the CTJ or the ATJ on the processes of the insulator flashover initiation in the presence of a high-voltage pulse. To generate these charged particles, a focused pulsed laser beam with a wavelength of 213 nm was used to irradiate the stainless steel electrodes in the vicinity of either the CTJ or ATJ.

II. EXPERIMENTAL SETUP

The experimental setup is shown in Fig. 1. The Marx generator[2] produced a positive polarity high-voltage pulse with amplitudes up to 300 kV and rise time of ~30 ns, which was applied over the dielectric sample located between two 130 mm-diameter highly polished stainless steel electrodes. We most frequently used cylindrical insulator samples 50 mm in diameter and 15 mm in length made of ULTEM (ULTEM is the commercial name of unfilled Polyetherimide, PEI). A turbo-molecular pump maintained the background pressure in the experimental stainless steel chamber at ≤6.5 mPa. The voltage waveforms were measured by a resistive voltage divider.

The surface flashover initiated by a laser beam generated by a NL303HT laser (EKSPLA) was registered with a fast framing 4QuikE intensified camera (Stanford Computer Optics) having a frame duration of 2 ns. The laser was equipped at its output with a fifth (FiH, $\lambda = 213$ nm) harmonic generator (H300FiHC) placed outside the laser head in an auxiliary harmonics generator module. The laser produced pulses have an energy of ~15 mJ and duration of ~5 ns at Full Width Half Maximum (FWHM) when the Q-switch was triggered at 255 μs relative to the beginning of the flash lamp's operation.

The laser beam average energy per second was measured by using a calibrated Ophir 12 A-P-SH power meter and a fast FDS100 Si photo-diode. The latter obtained a small part of the scattered laser beam power, which was used to control the relative reproducibility in the laser beam power for each laser shot. Using two EKSMA Optics mirrors (energy threshold ~0.2 J/cm^2 at $\lambda = 213$ nm) coated to decrease reflection and a lens with $f = 400$ mm (at $\lambda = 355$ nm), the laser beam (Gaussian-like energy radial distribution with diameter ~5 mm at FWHM) was focused through a quartz window at the desired location in the experimental chamber. The theoretical size of the laser beam at the focal plane was calculated to be $w = (2f\lambda/\pi d) \approx 10\,\mu$m. However, we estimate the actual focused laser beam diameter to be $\leq 300\,\mu$m. This is because of the uncertainty in the focal length at $\lambda = 213$ nm estimated as $f(\lambda_{213\,\mathrm{nm}}) \approx f(\lambda_{355\,\mathrm{nm}})[(n(\lambda_{355\,\mathrm{nm}}) - 1)/(n(\lambda_{213\,\mathrm{nm}}) - 1)] \approx 36.2$ cm, where $n(\lambda_{355\,\mathrm{nm}}) \simeq 1.565$ and $n(\lambda_{213\,\mathrm{nm}}) \simeq 1.625$ are the indices of refractions at 355 nm and 213 nm, respectively, and limitations in the spatial resolution (~60 μm/pixel) of the 4QuikE camera in the present experimental setup.

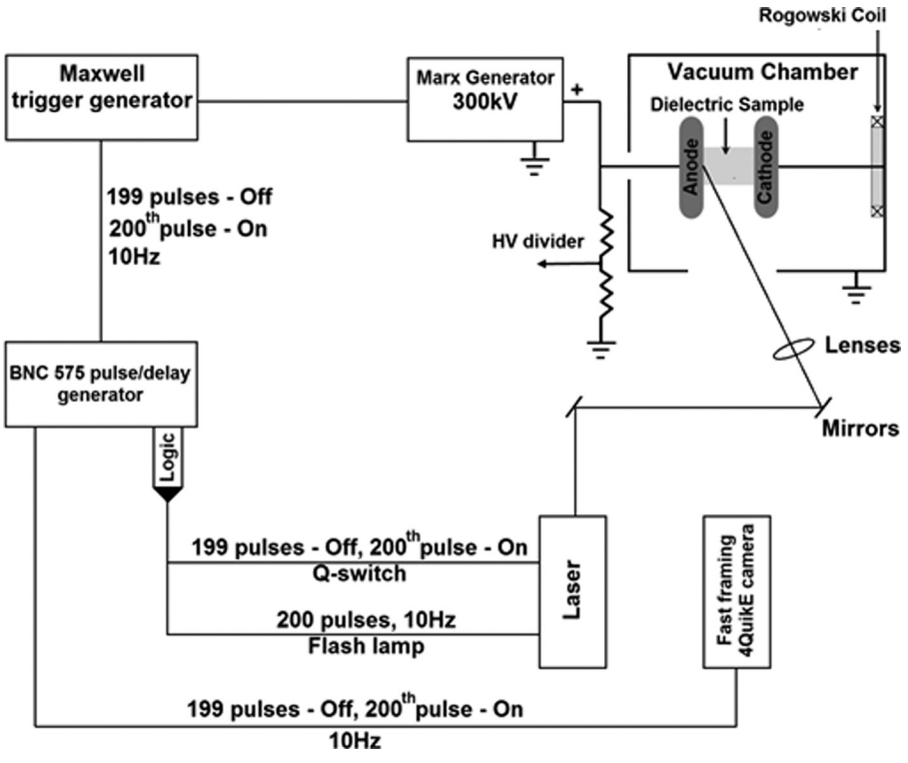

FIG. 1. Scheme of the experimental setup.

The operation of the laser, Marx generator, and 4QuikE camera was synchronized using the scheme shown in Fig. 1. The laser flash lamp was operated in the external burst mode of 200 flashes with a repetition rate of 10 Hz. At the 200th flash, the synchronization TTL pulses with variable time delay in the range $\tau_d = 250\ \mu$s–$420\ \mu$s with respect to the beginning of the flash lamp's operation were applied to the Q-switch and the triggering scheme of the Marx generator and the 4QuikE camera using different output channels of the BNS 575 pulse/delay generator. This scheme allows the time delays between the Q-switch and the Marx generator and the 4QuikE camera operation to be changed separately. The output power of the laser depends on the time delay of the Q-switch (Pockels cell) triggering with respect to the beginning of the flash lamp operation. Indeed, the laser is pumped (to achieve inverse population) using intense radiation flux generated by the gas discharge in the flash lamp. The latter is produced by the discharge of the storage capacitor with the half period of $\sim 500\ \mu$s. The intensity of the radiation and the level of population inversion change in time according to the time dependent amplitude of the discharge current. The maximum level of population inversion is at $\sim 250\ \mu$s relative to the beginning of the discharge current through the flash lamp. Correspondingly, by triggering the Q-switch at this time delay, one obtains the maximum energy of the laser beam which for the fundamental radiation (1064 nm) of the NL301G laser is 242 mJ. A BNC time delay generator was used to change the time delay between the beginning of the flash lamp operation and the triggering of the electronic circuit controlling the operation of the Q-switch. The latter allows us to change the energy of the fundamental laser radiation from its maximum value to almost zero. The conversion efficiency to the 5th harmonics depends strongly (non-linearly) on the power of the fundamental laser beam. Therefore, already at time delays $>400\ \mu$s of the Q-switch operation, the output energy of laser beam with $\lambda = 213$ nm becomes negligibly small and unstable.

III. EXPERIMENTAL RESULTS

The illumination of a stainless steel electrode with a high power density laser beam at $\lambda = 213$ nm can lead to two primary phenomena, namely, electron photo-emission and plasma formation. The laser threshold power density necessary for plasma formation at the surface of the stainless steel depends on the laser wavelength and duration and the quality of the metal surface. For $\lambda = 213$ nm and a 5 ns laser pulse duration, the threshold power density can be varied in the range 10^7–10^8 W/cm^2.[24–26] The threshold for electron photo-emission for stainless steel is in the range[27,28] 4.2–4.7 eV, which is less than the energy of a laser quanta $E_\gamma = hc/\lambda = 5.83$ eV, where h and c are Planck's constant and the speed of light, respectively.

In order to determine the power density threshold necessary for plasma formation in our experimental setup, several calibration experiments were conducted. First, using an Ophir power meter placed in the focal plane of the laser beam inside the stainless steel vacuum chamber, we measured the power of the beam versus the time delay of the Q-switch operation relative to the beginning of the flash lamp discharge. This dependence is shown in Fig. 2. Assuming that the diameter of the laser focal spot was 0.3 mm, we calculate the power density to be in the range 3.5×10^9–5.3×10^5 W/cm^2 for the time delay range $\tau_d = 262$–$387\ \mu$s. Note that for $\tau_d \geq 387\ \mu$s, the sensitivity of the Ophir power meter does not allow a reliable power measurement of the laser beam to be obtained. However, based on relative laser beam intensities obtained by the photodiode, we estimated the power density at those time delays (see Fig. 2, crossed circles). The increased error in the power density for $\tau_d \geq 387\ \mu$s is related to the non-reproducibility in laser operation at such small power levels of optical pumping.

Next, we designed a low-inductance Faraday cup (50 Ω load) with a polished stainless steel collector (diameter of 10 mm) placed inside the vacuum stainless steel chamber at the focal plane of the laser. A biased negative voltage of −400 V was applied to this collector with respect to the stainless steel grid (70% transparency) located in front of the collector at a distance of 1 mm. Using this setup, the electron photo-emission current $I_e(t)$ and total number of emitted electrons $N_e = e^{-1}\int_0^{t_p} I_e(t)dt$ were determined versus the time delay of the Q-switch operation, i.e., versus the laser beam power density. These dependencies are shown in Fig. 2. The photo-emission current data, and correspondingly, the total number of emitted electrons shown in Fig. 2 for $\tau_d \geq 387\ \mu$s are the average over 64 laser shots. The dependencies obtained allow us to estimate the quantum efficiency of electron photo-emission to be $\sim 3 \times 10^{-3}$%.

One can see that at laser beam power densities of $\omega \geq 5 \times 10^7$ W/cm^2, one starts to obtain a deviation in the linear increase in the amplitude of the emitted electron current. This deviation is not related to photo-electron emission and it can be explained by the space-charge effect. Indeed, for a 1 mm grid-collector gap, one can estimate the space-charge limited electron current density as ~ 1.9 A/cm^2 corresponding to ~ 1.35 mA considering electron emission from a focal spot of 0.3 mm in diameter. An increase in the amplitude of the emitted current above its space-charge limited value can be explained by the non-zero velocity of the emitted electrons, the non-planar geometry formed by the spot-like electron source, and the formation of plasma and its

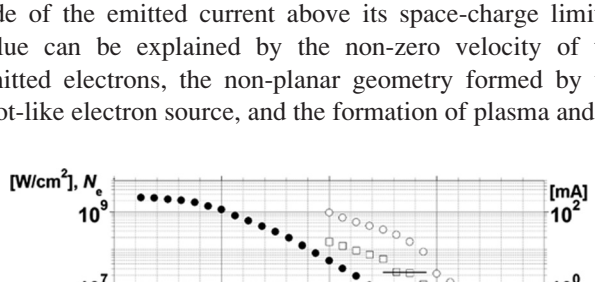

FIG. 2. Dependencies of the laser beam power density, electron photo-emission current amplitude, and total number of emitted electrons versus the time delay in the Q-switch operation. The Child space-charge limited electron current at a voltage of −400 V applied to the Faraday cup collector is also denoted.

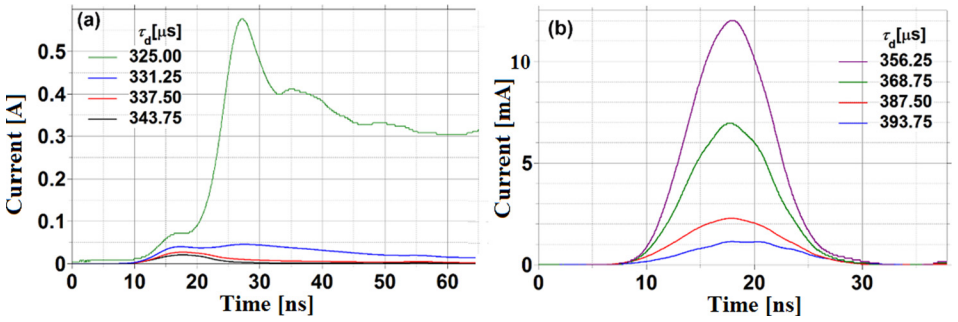

FIG. 3. Typical waveforms of the electron photo-emission currents versus the time delay in Q-switch operation.

expansion, which leads to an increase in the emitting surface area and decrease in the effective gap between the plasma boundary and the anode grid. In addition, one can see that at $\tau_d \geq 387\ \mu s$, when the energy of the laser beam becomes non detectable, a significant photo-electric current is still detected.

In addition, these experiments allow one to obtain the power density threshold necessary for the plasma formation at the surface of the stainless steel collector of the Faraday cup. In Fig. 3, typical waveforms of the electron photo-emission current are shown for different values of τ_d. It can be seen that the duration of the electron current pulse does not exceed ~10 ns at FWHM at time delays >350 μs corresponding to laser beam power densities $\leq 5 \times 10^7\ W/cm^2$, which coincides approximately with the duration of the laser beam measured by the photo-diode. However, an increase in power density leads to the appearance of a long (tens of nanoseconds) tail in the waveform of the electron current. Moreover, at power densities $\geq 5 \times 10^8\ W/cm^2$, one obtains that the amplitude of this tail becomes significantly larger than the first peak related to the photo-emission current. This phenomenon can be explained by the formation of the plasma at the surface of the stainless steel collector at a laser power density $\geq 5 \times 10^8\ W/cm^2$. This plasma serves as a source of electrons and the density, temperature, and consequently, the expansion velocity of this plasma increases with the increase in the power of the laser beam. Thus, for our experimental conditions, we show that to generate plasma at the surface of the stainless steel electrode, the laser power density threshold is $\geq 5 \times 10^7\ W/cm^2$.

Next, experiments using a ULTEM cylindrical insulator (90° insulator surface inclination relative to the conductor surface) were conducted. The average breakdown electric field, ~165 kV/cm, for this dielectric sample was determined by a conditioning method in our earlier research (see Ref. 2). In the present experiments, when the laser beam was focused at a location on the cathode electrode close to the CTJ, the amplitude of the output voltage of the Marx generator was ≤90 kV, corresponding to an average electric field of 60 kV/cm, i.e., almost three times lower than the breakdown electric field. Indeed, without the laser beam, no flashover occurs for several tens of voltage pulse applications. However, even the application of the laser beam with a power density as low as $\sim 10^5\ W/cm^2$ caused flashover of the insulator with a time delay of ~100 ns relative to the laser irradiation. Typical waveforms of the voltage and synchro-pulses of the 4QuikE camera and photo-diode pulse are shown in Fig. 4. Note that this laser power density is far below the power density threshold necessary for plasma formation at the surface of the stainless steel electrode. Thus, flashover was caused by primary photo-emitted electrons when their total number did not exceed $\sim 2 \times 10^7$. Such flashover was also obtained at the lowest possible Marx generator output voltage amplitude corresponding to an average electric field of 35 kV/cm. In the inset in Fig. 4, one can see a typical frame of the light emission from the plasma formed along the propagation route parallel to the insulator surface of the primary photo-electrons generated by the laser beam illumination of the cathode surface in the vicinity of the CTJ. The relatively long time delay between the formation of the primary electrons and the appearance of the flashover is the result of the very low laser power density. An increase in the power density of the laser beam leads to a decrease in this time delay and at $\geq 10^6\ W/cm^2$ ($N_e \geq 2 \times 10^8$), the flashover was obtained almost simultaneously with the laser irradiation.

For the same applied voltage and a much higher laser power density applied near the ATJ (as high as $2 \times 10^9\ W/cm^2$ in Fig. 5(a)), no flashover develops. Flashover does develop from the ATJ only for applied voltages ≥150 kV at a laser power density $>5 \times 10^9\ W/cm^2$. The laser beam of such a power density generates a sufficiently large expanding plasma volume, which serves as a source of ions and UV that can initiate a surface flashover near the ATJ. Indeed, the obtained waveforms of the voltage showed a time delay of up to 300 ns

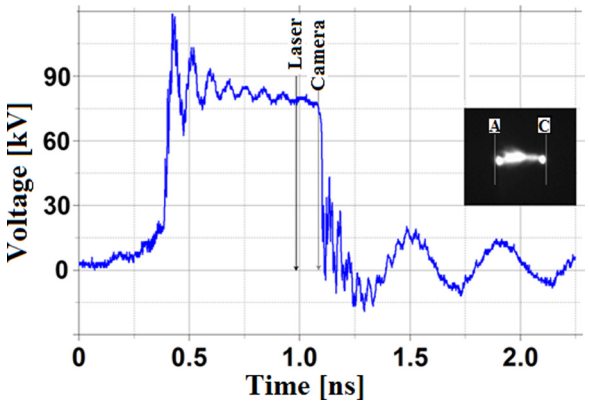

FIG. 4. The voltage waveform across the insulator. The arrows indicate the starting time of the laser beam followed by the synchro-pulse of the 4QuikE camera (frame duration 2 ns, camera amplification 850 V). Inset: light radiation from the surface flashover plasma. Here, the laser beam is applied in the vicinity of the CTJ of a 1.5 cm-long cylindrical sample. The applied voltage amplitude is 90 kV and the laser beam power density is $\sim 10^5\ W/cm^2$.

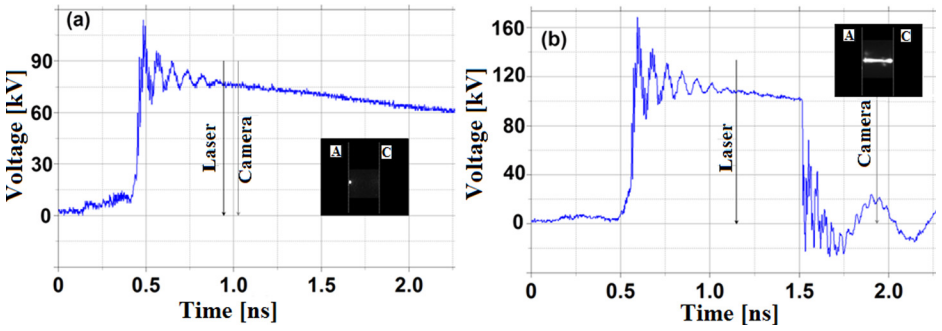

FIG. 5. Same as Fig. 4 but here, the laser beam is applied in the vicinity of the ATJ with a laser beam power density of $\sim 2 \times 10^9$ W/cm^2 and applied voltage amplitude of 90 kV in (a) and 5×10^9 W/cm^2, 150 kV, respectively, in (b). Inset: light emission from the plasma formed at the anode electrode surface as a result of irradiation by the laser beam. Frame duration is 2 ns, camera amplification is 700 V.

between the beginning of the flashover and the laser beam illumination of the anode (Fig. 5(b)).

The results of these experiments support our previous work[1–3] in that they show that a small amount of primary electrons produced near the CTJ is sufficient to produce vacuum insulator surface flashover if the electric field accelerates them along this surface. If conditions exist that sufficient plasma forms at the ATJ and there is sufficient time and power for it to expand, acquire the anode potential, and shorten the anode cathode gap, flashover may develop. The latter though, is the result of the focused high power density of the laser at the ATJ and does not mimic the natural development of most vacuum insulator breakdown processes.

We also tested 15 mm-long ULTEM samples having surfaces inclined at 45° relative to the cathode. In this case, the flashover electric field without laser beam application was ~300 kV/cm.[2] When the laser beam was focused in the vicinity of the ATJ, no flashover was obtained even for the largest possible laser beam power density and voltage pulse amplitudes up to 180 kV. In addition, no flashover was obtained when the laser beam was focused to the vicinity of the CTJ with power densities similar to those that caused flashover for cylindrical insulators (see Fig. 4). Only when the laser beam power density was increased to 2×10^7 W/cm^2, insulator flashover occurs at an applied voltage of 90 kV. However, even at this power density, not all the shots resulted in flashover. This laser power density value is close to that necessary for plasma formation at the surface of the stainless steel electrode. An increase in laser power density leads to reliable flashover of the insulator but with a significant time delay (>100 ns) relative to the application of the laser beam. Typical framing images of the light emission from the flashover plasma are shown in the inset in Fig. 6. One can see that the discharge channel is not exactly opposite to the flashover plasma channel obtained in the case of the cylindrical insulator flashover.

Finally, we conducted a set of experiments in which the laser beam was focused at the middle of the cylindrical insulator with an applied voltage of 90 kV. The results of these experiments showed that at a laser power density $\geq 2 \times 10^7$ W/cm^2 for some generator shots, one starts to obtain insulator flashover but with time delays of >300 ns relative to the laser beam. Let us note that we do not know whether this power density is sufficient to generate plasma at the surface of the insulator, but the energy of quanta should be sufficient to cause intense electron photo-emission.[29] An increase in the laser power density led to a decrease in this time delay to ~100 ns, but even at 10^9 W/cm^2, some shots without insulator flashover were obtained. Typical waveforms of the voltage and framing images of the light emission of the flashover plasma are shown in Fig. 7. One can see in Fig. 7(a) that the flashover begins from the mid location on the insulator surface illuminated by the laser beam, but the voltage across the insulator does not short. For the same conditions, full flashover is observed together with shorting in Fig. 7(b). This suggests that the discharge plasma channel crosses first the "anode" part of the insulator and then the discharge from the cathode side begins. The latter can be explained by the fact that the flashover plasma acquires the anode potential and the effective gap decreases two-fold, which leads to an increase in the average electric field along the "cathode" part of the insulator above its threshold value.

IV. SUMMARY

The application of a short duration UV laser beam pulse at a wavelength of 213 nm allows photo-electron emission to be produced from the stainless-steel electrode in the vicinity of the CTJ and ATJ when the beam is focused at these locations. When the applied electric field orientation causes the electrons to accelerate along the surface of the insulator, a small current of photo-emitted electrons (>1 mA) is sufficient to initiate vacuum insulator surface flashover at electric fields several times smaller than that required to achieve flashover without laser illumination. Illumination near the ATJ, resulting in photoelectrons only, causes no flashover

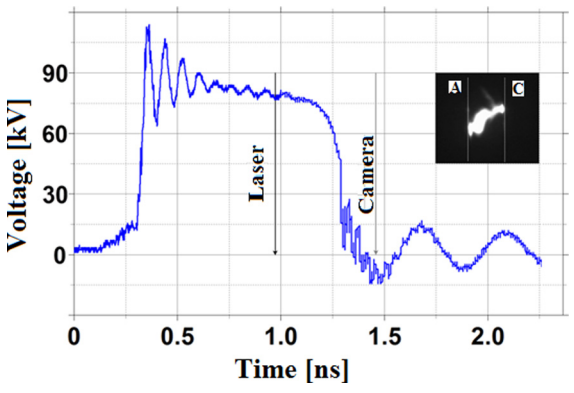

FIG. 6. The voltage waveform across the insulator inclined at 45°. The arrows indicate the starting time of the laser beam and synchro-pulse of the 4QuikE camera (frame duration 2 ns, camera amplification 650 V) application. Inset: light radiation from the surface flashover plasma. The laser beam is applied in the vicinity of the CTJ of sample inclined at 45°. The applied voltage amplitude is 90 kV and the laser beam power density is $\sim 5 \times 10^7$ W/cm^2.

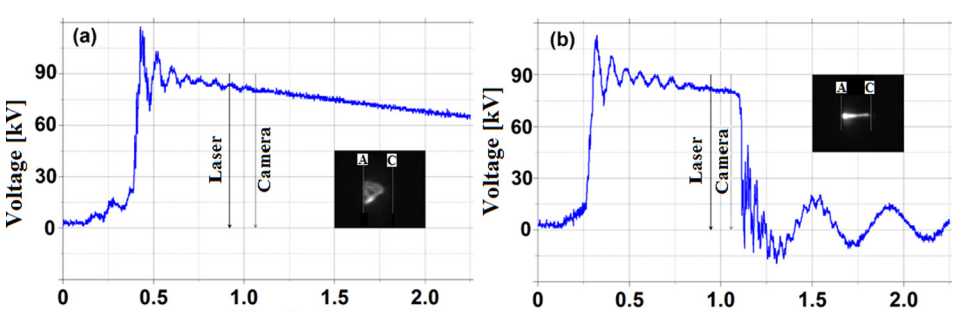

FIG. 7. The voltage waveform across the cylindrical insulator. The arrows indicate the starting time of the laser beam and synchro-pulse of the 4QuikE camera (frame duration 3 ns, camera amplification 750 V) application. Inset: light radiation from the surface flashover plasma. The laser beam is applied in the middle of the insulator. The applied voltage amplitude is 90 kV and the laser beam power density is $\sim 10^9$ W/cm^2.

even at average electric fields of 100 kV/cm. Only sufficient plasma formation at the anode electrode surface with increased laser beam power leads to the insulator surface flashover. For an insulator surface inclined at 45° relative to the cathode, no flashover occurs when the anode triple junction is illuminated, although the electric field at that location is theoretically infinite. Finally, experiments using laser beam irradiation of the insulator surface at the middle of the anode-cathode gap showed that the surface discharge propagates first from the irradiated location toward the anode, and only when the discharge plasma channel crosses the "anode" part of the insulator, the discharge from the cathode side begins.

ACKNOWLEDGMENTS

The authors are grateful to E. Flyat and S. Gleizer for technical assistance in experiments. This work was supported by an RSF (Rafael Science Fund) grant. This fund was established to enhance scientific research collaboration between industry and academic institutions.

[1]J. G. Leopold, C. Leibovitz, I. Navon, and M. Markovits, Phys. Rev. ST Accel. Beams **10**, 060401 (2007).
[2]J. Z. Gleizer, Ya. E. Krasik, U. Dai, and J. G. Leopold, IEEE Trans. Dielectr. Electr. Insul. **21**, 2394 (2014).
[3]J. Z. Gleizer, Ya. E. Krasik, and J. G. Leopold, J. Appl. Phys. **117**, 073301 (2015).
[4]H. C. Miller, IEEE Trans. Electr. Insul. **24**, 765 (1989).
[5]I. Smith, IEEE Trans. Plasma Sci. **34**, 1585 (2006).
[6]S. Humphries, *Principles of Charged Particle Acceleration* (Wiley, New York, 1989).
[7]N. M. Jordan, Y. Y. Lau, D. M. French, R. M. Gilgenbach, and P. Pengvanich, J. Appl. Phys. **102**, 033301 (2007).
[8]W. A. Stygar, J. A. Lott, T. C. Wagoner, V. Anaya, H. C. Harjes, H. C. Ives, Z. R. Wallace, G. R. Mowrer, R. W. Shoup, J. P. Corley, R. A. Anderson, G. E. Vogtlin, M. E. Savage, J. M. Elizondo, B. S. Stoltzfus, D. M. Andercyk, D. L. Fehl, T. F. Jaramillo, D. L. Johnson, D. H. McDaniel, D. A. Muirhead, J. M. Radman, J. J. Ramirez, L. E. Ramirez, R. B. Spielman, K. W. Struve, D. E. Walsh, E. D. Walsh, and M. D. Walsh, Phys. Rev. ST Accel. Beams **8**, 050401 (2005).
[9]R. A. Anderson, "Review of surface flashover theory," in *Proceedings of the XIVth International Symposium Discharges and Electrical Insulation in Vacuum, Santa Fe, NM, September 1990* (IEEE, 1990), pp. 1–15.
[10]E. J. Lauer and M. A. Lauer, "Particle acceleration devices with improved geometries for vacuum-insulator-anode triple junctions," Patent no. 9,089,039 B2 (21 July 2015).
[11]K. Morales, J. Krile, A. Neuber, and H. Krompholz, IEEE Trans. Dielectr. Electr. Insul. **13**, 803 (2006).
[12]J. Krile, G. Edmiston, K. Morales, A. Neuber, H. Krompholz, and M. Kristiansen, Laser Phys. **16**, 194 (2006).
[13]J. Krile, A. Neuber, and H. Krompholz, Appl. Phys. Lett. **89**, 201501 (2006).
[14]J. Krile, A. Neuber, J. Dickens, and H. Krompholz, IEEE Trans. Plasma Sci. **33**, 1149 (2005).
[15]J. T. Krile, A. A. Neuber, and H. G. Krompholz, IEEE Trans. Plasma Sci. **36**, 332 (2008).
[16]C. L. Enloe and R. M. Gilgenbach, Plasma Chem. Plasma Process. **7**, 89 (1987).
[17]C. L. Enloe and R. M. Gilgenbach, IEEE Trans. Plasma Sci. **16**, 379 (1988).
[18]C. L. Enloe and R. M. Gilgenbach, IEEE Trans. Plasma Sci. **17**, 550 (1989).
[19]L. Xu, J. Deng, and M. Wang, IEEE Trans. Plasma Sci. **40**, 3508 (2012).
[20]L. Xu, J. Deng, and M. Wang, IEEE Trans. Dielectr. Electr. Insul. **20**, 706 (2013).
[21]J. B. Javedani, T. L. Houck, D. A. Lahowe, G. E. Vogtlin, and D. A. Goerz, in Proceedings of the 17th IEEE International Pulsed Power Conference, Washington, DC, 28 June 2009.
[22]Z.-B. Wang, Y.-H. Cheng, and K. Wu, IEEE Trans. Dielectr. Electr. Insul. **18**, 561 (2011).
[23]L. Xu, M. Wang, F. Li, Z. Yang, and J. Deng, "Spectroscopic study of surface flashover under pulsed voltage in vacuum," IEEE Trans. Plasma Sci. (published online 2015).
[24]S. I. Anisimov, Ya. A. Imas, G. S. Romanov, and Yu. V. Khodyko, *Interaction of High-Power Radiation With Metals* (Nauka, Moscow, 1970) (in Russian).
[25]S. A. Akhmanov, V. I. Emel'yanov, N. I. Koroteev, and V. N. Seminogov, Sov. Phys. Usp. **28**, 1084 (1985).
[26]S. I. Anisimov and B. S. Lukyanchik, Sov. Phys. Usp. **45**, 293 (2002).
[27]M. Wisse, L. Marot, B. Eren, R. Steiner, D. Mathys, and E. Meyer, Fusion Eng. Des. **88**, 388 (2013).
[28]A. Gruszecka, M. Szymanska-Chargot, A. Smolira, J. Cytawa, K. Gluch, and L. Wojcik, Nucl. Instrum. Methods Phys. Res. B **311**, 116 (2013).
[29]D. K. Davies, Br. J. Appl. Phys. (J. Phys. D) **2**, 1533 (1969).